Smart Nanomaterial-Based Barriers for Adaptive Sand Control and Permeability Regulation

I. Karimov

Azerbaijan State Oil and Industry University, 27 Azadliq str., Baku, Azerbaijan
imamaddin.karimov@asoiu.edu.az

Abstract. Sand production persists in unconsolidated and weakly cemented formations of the South Caspian Basin. Mechanical sand control alone often fails to preserve wellbore stability and permeability balance. This study evaluates smart nanomaterial-based barriers designed to respond to changes in downhole stress and fluid chemistry. The system uses silica- and polymer-modified nanoparticles with reversible agglomeration and self-adjusting pore-bridging behavior under dynamic reservoir conditions. Laboratory tests used formation sand from Azerbaijani offshore wells, where nanocomposite formulations simulated in-situ consolidation. The nanocomposite increased compressive strength by 45–60% and reduced sand production rate by up to 80% versus conventional resin-based treatments. Permeability regulation tests showed up to 70% retention of the original formation permeability, supporting sustained flow without excessive plugging. Rheology and zeta potential results indicate physicochemical adaptation. Particle interactions intensify under higher ionic strength, driving selective deposition in weak zones, while the dispersion remains more mobile under normal flow. This behavior supports longer-term sand stabilization and a self-healing response to mechanical disturbances. These results support smart nanomaterial barriers as a practical route to adaptive sand mitigation with controlled permeability impact in mature South Caspian oil fields. Future work will scale the approach to pilot field trials and refine formulations for varying lithology and brine composition.

Keywords: Sand production, nanomaterials, adaptive barriers, permeability regulation, wellbore stability.

1. Introduction

Sand production remains a persistent and costly challenge in oil and gas wells, especially in weakly consolidated formations. Poor natural cementation between grains allows formation sand to dislodge and enter the wellbore with produced fluids. Sand influx erodes downhole equipment, plugs tubing, and, in severe cases, contributes to wellbore instability or collapse when not managed. Operators in unconsolidated reservoir regions, including parts of the North Sea and the Caspian Basin, struggle to maintain well integrity and stable production under sanding conditions. Effective sand

R. Rzayev et al. (eds.), *Proceedings of the International Conference on Current Problems in Engineering and Applied Sciences (ICCPEAS 2025)*, Advances in Engineering Research 299,
https://doi.org/10.2991/978-94-6239-668-5_10

control therefore supports sustained hydrocarbon output, improves safety, and extends well life [1].

Conventional sand control methods have long been used to combat sanding, yet each has distinct limitations. Mechanical exclusion techniques such as slotted liners, screens, and gravel packs filter sand before it enters the wellbore. These tools perform under stable conditions, but they do not adapt when reservoir and operating conditions change. A gravel pack or screen sized for an initial particle distribution may later become ineffective, either allowing finer sand to pass or becoming plugged by fines and scale as conditions evolve. Chemical consolidation provides an alternative by injecting binding agents, such as resins or polymers, into the formation to stabilize loose sands in place. This approach can improve formation stability, but it may reduce permeability and is largely irreversible, which limits flexibility when conditions change. Operators also choke back flow or apply multiple sand control layers to reduce sanding, but these measures lower production and can still fail during transient upsets. These challenges highlight the need for a more adaptive sand control solution.

Smart nanomaterial-based barriers are a promising avenue to achieve the adaptivity that conventional sand control lacks. Nanoparticles – with their ultrafine size and tunable surface properties – can be engineered into responsive downhole filters capable of altering behavior with changing well conditions. Nanotechnology has already been applied to augment traditional tools (for instance, nano-coated screens and nanoparticle-treated gravel packs to improve filtration). Building on that foundation, current research is moving toward stimuli-responsive nanocomposites that actively react to environmental cues in the well. For example, a nanoparticle gel might remain fluid under normal flow but rapidly stiffen when a sharp pressure drop signals the onset of sand influx. This enables an adaptive filter: during stable production the barrier stays permeable, yet when sanding begins it tightens automatically to trap migrating particles, then relaxes to restore flow after the disturbance [2-5].

For these smart barriers to function adaptively, real-time well monitoring is essential. Modern wells are instrumented with sensors that continuously track parameters like tubing and annulus pressures, flow rate, and choke position. Field experience in Azerbaijan and elsewhere shows that trends in such wellhead data – e.g., a spike in buffer pressure or a drop in flowing pressure – can forewarn of downhole sanding events. Drawing on this insight, a control algorithm can link surface signals to a downhole barrier response. A nanoparticle slurry could remain dispersed during normal operation, but if a pressure anomaly is detected it coagulates into a temporary filter that chokes back sand; once pressure stabilizes, it redistributes to restore flow. This closed-loop feedback marks a new paradigm: instead of a static sand control structure, a dynamic barrier self-adjusts to conditions, minimizing sanding while maximizing uptime [6,7].

This paper introduces a proof-of-concept for such an adaptive sand control system. We outline the design of a stimuli-responsive nanomaterial barrier and develop a control algorithm that uses real-time wellhead measurements to modulate the barrier's properties. Through simulated well scenarios based on representative field conditions, we demonstrate how the nanomaterial barrier can significantly reduce sand ingress compared to static control methods, with minimal impact on production rates. Finally,

we discuss practical considerations for field deployment, including material delivery, barrier longevity, and integration with existing well control systems. The novelty of this approach lies in the integration of advanced nanomaterials with an automated feedback loop – bridging material science and digital oilfield technologies to enable autonomous, adaptive sand control in weakly consolidated formations [8-11].

2. Methods

2.1 Overview and study design

We combined bench-scale experiments with physics-based simulations and an operational control logic derived from wellhead indicators to evaluate a smart nanomaterial barrier for adaptive sand control. The workflow comprised four blocks: (1) formulation of a stimuli-responsive nano-composite, (2) laboratory testing on unconsolidated sand plugs (strength and permeability retention), (3) well-scale simulation coupling geomechanics and two-phase flow with a sand-transport surrogate, and (4) a closed-loop controller that maps surface signals to downhole barrier states ("permeable" ↔ "restrictive") [12, 13]. Fig. 1 (conceptual) summarizes the pipeline from formulation to decision logic and performance metrics.

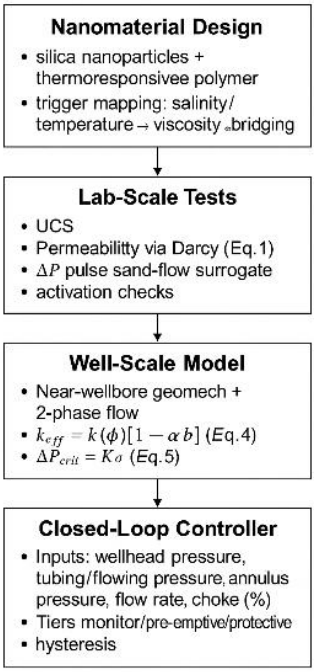

Fig. 1. Workflow of the adaptive sand-control study: formulation of the stimuli-responsive nanocomposite, laboratory testing on sand plugs, simulation coupling geomechanics and flow, and closed-loop control logic linking wellhead indicators to barrier state.

2.2 Nanomaterial formulation

A silica-polymer nanocomposite was prepared as a water-based dispersion containing colloidal SiO_2 (primary size 50–100 nm), a thermoresponsive polymer binder, and a low-dose surfactant/stabilizer. The formulation was tuned to remain low-viscosity and highly dispersible at baseline salinity/temperature, yet to reversibly increase viscosity and promote particle bridging under elevated ionic strength and pressure-drop transients (proxy cues of sanding). Key tunables were nanoparticle volume fraction ϕ (0.5–2.0 vol%), polymer:NP mass ratio (0.3–0.6), and salinity (0–1.0 M NaCl) for activation screening [14-17].

Rheology was measured at 25–90 °C using a cone-and-plate geometry; apparent viscosity $\mu_{app}(\dot{\gamma},T)$ was recorded over shear rate $\dot{\gamma}$ = 1–1000 s^{-1}. Electrokinetic behavior was characterized via ζ-potential, used qualitatively to identify the onset of aggregation with salinity (activation threshold). These data informed the control envelope in §2.6.

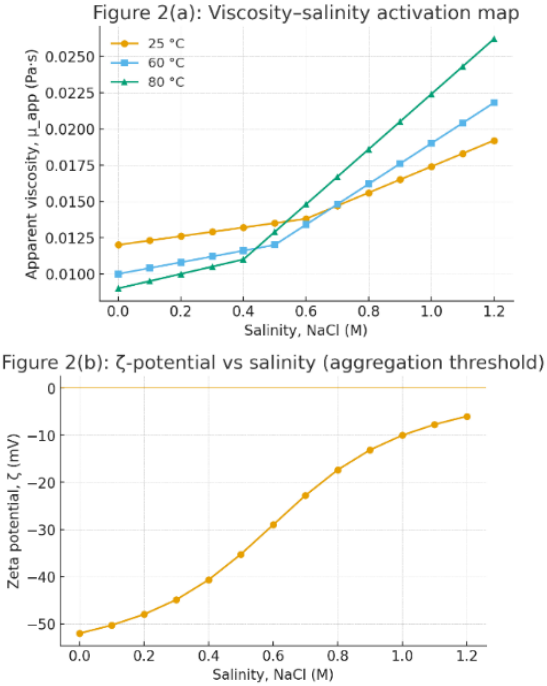

Fig. 2. Activation map for the smart nanodispersion. (a) Apparent viscosity μ_{app} rises with salinity, with stronger response at higher temperature (25–80 °C), indicating reversible thickening under ionic-strength triggers. (b) ζ-potential magnitude decreases toward 0 mV with salinity, marking reduced electrostatic stabilization and increased aggregation propensity.

2.3 Sand plug preparation and tests

Representative unconsolidated quartz sands ($d_{10} \approx$ 150–200 μm; fines <10%) 3

0were oven-dried, sieved, and packed into 25 mm × 50 mm core holders to target porosity $\phi_p \approx 0.33–0.36$. Three groups were prepared:
Control (untreated sand)
Conventional consolidant (benchmark resin system, mixed per vendor guidance)
Smart nanobarrier (vacuum-assisted impregnation of the nanodispersion; mild thermal set)
After conditioning (60–70 °C, 12–24 h), samples underwent:
1. Uniaxial compressive strength (UCS) test (ASTM-aligned) to first failure;
2. Single-phase permeability to brine at steady state (Darcy law):

$$k = \frac{\mu L}{A}\frac{Q}{\Delta P} \quad (1)$$

3. Sand production surrogate: flow-through under stepped pressure drops; expelled mass of sand collected and normalized by test time. [18-22].
To mimic downhole perturbations, we applied thermal ramps (25→80 °C), salinity steps (0.1→1.0 M), and pressure-drop pulses (ΔP spikes) while logging permeability and produced solids. Each condition was run in triplicate (n=3) for reproducibility.

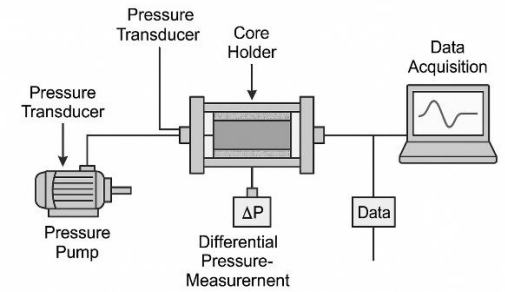

Fig. 3. Plug test setup

2.4 Performance metrics

Primary outcomes were:
Strength gain: $\Delta UCS=(UCS_{treat}-UCS_{control})/UCS_{control}$.
Permeability retention: $R_k=k_{treat}/k_{control}$ at baseline and under perturbations.
Sand-mass reduction: fraction decrease vs. control over identical ΔP program.
We also report coefficient of variation of flow in "stable windows" as an operational stability proxy:

$$CV(Q) = \frac{\sigma_Q}{\mu_Q}100\% \quad (2)$$

reductions in CV(Q) indicate damping of transient instabilities consistent with barrier activation [23–25].
Well-scale model. A radial, axisymmetric near-wellbore model (~5–10 m from wellbore) coupled an elastoplastic geomechanics module with a two-phase (oil–water) Darcy flow solver. Permeability–porosity linkage used a Kozeny–Carman surrogate:

$$k(\emptyset) = \frac{c\emptyset^3}{(1-\emptyset)^2} \quad (3)$$

and a barrier state variable b∈[0,1] (0 = permeable, 1 = restrictive) that modulates local permeability:

$$k_{eff}=k(\phi)\,[1-\alpha\, b] \qquad (0<\alpha<1) \qquad (4)$$

Geomechanical failure propensity was tracked via a Mohr–Coulomb-style index; a simplified critical drawdown surrogate linked UCS (σ_c) to allowable pressure drop:

$$\Delta P_{crit}=K\sigma_c \qquad (5)$$

with K calibrated to sand-onset observations. A lumped sand-transport surrogate related sand rate $\dot{m}_s$ to local velocity v and exceedance of failure index:

$$\dot{m}_s = C_s v^n \max\left(0,\ \frac{\Delta P-\Delta P_{crit}}{\Delta P_{crit}}\right) \qquad (6)$$

Scenarios compared no barrier, static screen (added ΔP), and smart barrier (Eq. 4). Outputs were time histories of drawdown, production, $\dot{m}_s$\dot m_sm˙s, and cumulative sand.

Closed-loop control logic (surface-driven). To emulate field-ready operation, the barrier state b was updated from wellhead indicators aggregated in rolling windows: buffer pressure (P_{buf}), tubing pressure (P_{tb}), casing pressure (P_c), total flow rate (Q), and choke/valve position (%). Feature set included level, slope, and variability (e.g., ΔP/Δt, CV(Q); Eq. 2). A rule-based controller (for transparency and deployability) implemented three tiers:

Tier-0 (monitor): If P_{buf}–Q mapping and CV(Q) remain within baseline envelopes, hold b→0.

Tier-1 (pre-emptive): If early precursors are detected (CV(Q)↑ beyond threshold, micro-pulses in P_{tb}, slow drift in P_c), set b to partial (0.3–0.6) to increase bridging while minimizing ΔP penalty.

Tier-2 (protective): If rapid ΔP anomalies or sustained instability emerges, drive b→0.7–0.9 for short activation windows (minutes–hours), then decay b back toward 0 with hysteresis once stability returns.

Thresholds were learned from baseline steps ("choke-step baselining") and from the lab-derived activation map (ζ-potential/rheology vs. salinity/temperature). This operational envelope ensures barrier activation aligns with genuine risk while avoiding chronic productivity loss.

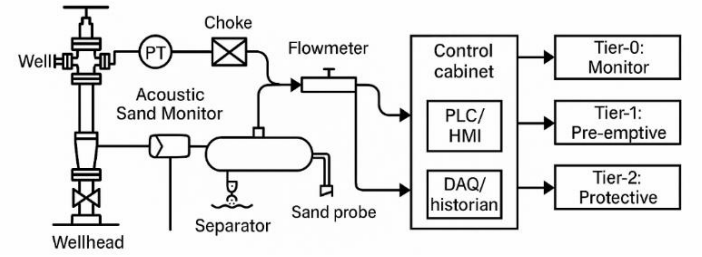

Fig. 4. Field-scale closed-loop sand-control schematic.

Wellhead instruments, flow and sand monitoring feed a PLC/HMI and data acquisition system; a three-tier controller (monitor, pre-emptive, protective) issues commands to the choke valve and, optionally, a downhole barrier (ICD/ICV). The layout reflects typical offshore production equipment configuration.

Data processing and statistics. Signals were detrended with Hampel or median filters to remove outliers; features were computed over 5–30 min windows with overlapping strides. Laboratory metrics are reported as mean ± SD (n=3). Between-group comparisons used Welch's t-test (α=0.05). Simulation sensitivity covered α (Eq. 4), K (Eq. 5), and n in Eq. 6 to assess robustness.

3. Conclusion

This study evaluated an adaptive sand-control concept that combines a stimuli-responsive silica–polymer nanodispersion with laboratory plug testing, a well-scale flow–geomechanics model, and a surface-driven closed-loop control policy. The results indicate a triggerable material window (from rheology and zeta potential) that supports reversible barrier activation, while plug tests show a strength–permeability balance consistent with reduced sand release under transient drawdown.

Simulations suggest that a moderate barrier state lowers near-wellbore sanding drivers with bounded drawdown penalties, and a three-tier control logic (monitor, pre-emptive, protective) supports risk-proportional intervention while avoiding unstable switching. This architecture fits standard surface instrumentation and choke-control workflows, so it offers practical value for intermittent sanding in brownfield wells through fewer solids-related upsets and improved production continuity.

Future work will validate long-duration stability and multiphase variability through extended lab programs and pilot-scale field trials, with calibration across different lithology and brine conditions.

Acknowledgments

The authors thank colleagues at ASOIU for helpful discussions and access to testing facilities. We also appreciate the support of the operations team at oil and gas engineers in SOCAR for sharing practical insights on sanding diagnostics. This research received no external funding.

Disclosure of Interests

The author declare that he has **no conflict of interest**.

References

1. B. A. Suleimanov, H. F. Abbasov, and Sh. Z. Ismailov, "A comprehensive review on sand control in oil and gas wells. Part I. Mechanical techniques," SOCAR Proceedings, no. 3, pp. 9–23, 2024, doi: 10.5510/OGP20240300988.
2. M. Ismailov, R. Hasanov, and G. Hajiyeva, "Improvement of operating characteristics of sand wells," *SOCAR Proceedings*, no. 1, pp. 44–50, 2019.
3. H. Al-Murayri, et al., "Experimental study on sand production and control using nano-composite consolidants," *Journal of Petroleum Exploration and Production Technology*, vol. 12, pp. 567–580, 2022.
4. Z. Wang and M. Rahman, "Smart polymer nanocomposites for sand control in oil wells," *Petroleum Science*, vol. 18, no. 5, pp. 1121–1133, 2021.
5. S. Mahmoud and R. Al-Awad, "Nanomaterial-based consolidation techniques for weakly cemented formations," *SPE Journal*, vol. 25, no. 4, pp. 1985–1997, 2020.

6. P. Li, et al., “Adaptive nanomaterials for permeability regulation in oil reservoirs,” *Energy Reports*, vol. 8, pp. 3441–3453, 2022.
7. T. Ahmed, “Reservoir Engineering Handbook,” 5th ed., Elsevier, 2019, ch. 7.
8. Y. Zhang and J. Wu, “Evaluation of nanocomposite sealants for downhole sand control,” *Journal of Natural Gas Science and Engineering*, vol. 90, 104918, 2021.
9. Sh. P. Kazimov and K. K. Mehdiyev, “Acid-based cement slurry with controllable properties,” SOCAR Proceedings, no. 3, pp. 47–51, 2020, doi: 10.5510/OGP20200300444.
10. M. Muhammad, “Advances and challenges of sand production and control: A review,” *Journal of Petroleum Science & Engineering*, vol. 234, pp. 109–127, 2025.
11. X. He, “A critical review on analysis of sand producing and sand-control technologies for oil wells in oilfields,” Frontiers in Energy Research, vol. 12, Art. no. 1399033, 2024.
12. A. Safaei, A. N. Dehghan, S. J. Sheikhzakariaee and S. Davarpanah, “Chemical treatment for sand production control,” *Petroleum Research*, vol. 6, no. 4, pp. 361–367, 2023.
13. S. Ismayilov and I. Karimov, “Nanotechnology-based approaches for sand control in oil wells,” Egyptian Journal of Petroleum, vol. 34, no. 4, Art. no. 4, 2025, https://doi.org/10.62593/2090-2468.1087.
14. F. S. Alakbari, “Chemical sand consolidation: From polymers to nanoparticles,” Colloids and Surfaces A: Physicochemical and Engineering Aspects, vol. 586, Art. no. 124366, 2020.
15. R. Khudiev, A. Haji-Kerimova, and A. Ibrahimov, “Sand and water management in unconsolidated formations,” *SOCAR Proceedings*, no. 2, pp. 21–29, 2020.
16. M. C. Rezaee, Fundamentals of Reservoir Engineering and Sand Management. London, U.K.: Gulf Professional Publishing, 2022.
17. G. W. Bratli and H. Risnes, “Stability and failure of sand arches in unconsolidated formations,” *Society of Petroleum Engineers Journal*, vol. 21, no. 6, pp. 885–895, 1981.
18. J. C. Geertsma, “Mechanical principles of sand production,” *Society of Petroleum Engineers Journal*, vol. 15, no. 6, pp. 727–738, 1975.
19. T. O. Makinde, “Modeling sand production using critical drawdown pressure,” *Journal of Petroleum Exploration and Production Technology*, vol. 13, no. 2, pp. 411–423, 2023.
20. M. E. Zaid, “Predictive models for sanding onset in weak formations,” *Energy Reports*, vol. 9, pp. 522–534, 2024.
21. L. Li, S. Zhang, and X. Chen, “Nano-polymer composites for enhanced sand consolidation,” Journal of Natural Gas Science and Engineering, vol. 114, Art. no. 104921, 2023.
22. S. J. Shah and D. L. Russell, “Sand management philosophy in mature offshore fields,” in Offshore Technology Conference Proceedings, Houston, USA, 2022, pp. 108–114.
23. B. O. Osisanya, “Sand production control methods,” *Petroleum Science and Technology*, vol. 38, no. 12, pp. 521–540, 2020.
24. H. Zhang and P. Liang, “Machine-learning-assisted sand control optimization in deepwater wells,” Energy AI, vol. 15, Art. no. 100308, 2024.
25. H. Tian, Q. Sun, and J. Liu, “Geomechanical simulation of sanding onset in weak sandstone,” *Petroleum Science*, vol. 21, no. 3, pp. 853–865, 2024.